

The Stewart–Lyth Inverse Problem

Eloy Ayón–Beato*, Alberto García†, Ricardo Mansilla*‡, César A. Terrero–Escalante§

Departamento de Física, CINVESTAV–IPN, Apdo. Postal 14–740, 07000, México D.F., México.

**Departamento de Física Teórica, IF–UNAM, Apdo. Postal 20–364, 01000, México D.F., México.*

Abstract

In this paper the Stewart–Lyth inverse problem is introduced. It consists of solving two non–linear differential equations for the first slow–roll parameter and finding the inflaton potential. The equations are derived from the Stewart–Lyth equations for the scalar and tensorial perturbations produced during the inflationary period. The geometry of the phase planes transverse to the trajectories is analyzed, and conclusions about the possible behaviour for general solutions are drawn.

I. INTRODUCTION

The analysis of observations of the Cosmic Microwave Background Radiation, recently reported by the experiments BOOMERANG and MAXIMA–1 [1,2], confirmed that, at present–day, inflation [3,4] still remains as the favourite model for the origin of structure in the Universe. The main reason is that the currently obtained observational data on structures in the Universe is interpreted in a natural way within the framework of the Gaussian adiabatic and nearly scale–invariant density perturbations that the usual models produce. On the other hand, it is one of the simplest paradigms within which rigorous theoretical predictions can be achieved.

However, the inflationary paradigm is quite a broad one, and there are several equally satisfactory implementations of the inflationary idea. The simplest scenario arises when the dynamics of inflation (both classical and quantum) are dominated by a single scalar field (inflaton) evolving in a nearly flat potential. Even in this case, there is a large number of candidates for the potential. For this scenario it is well established [5,6] that, to a good approximation, the scalar and tensor perturbations will take on a power–law form, with the tensor ones giving a sub–dominant (and almost negligible) contribution. A way

*E-mail: ayon@fis.cinvestav.mx

†E-mail: aagarcia@fis.cinvestav.mx

‡E-mail: mansy@servidor.unam.mx

§E-mail: cterrero@fis.cinvestav.mx

of discriminating between candidates for inflationary potential is the comparison between observed and predicted perturbations spectra. However, the present level of accuracy of the observations is well below the accuracy of the predictions for most of the models [7], allowing a still large number of them to remain as candidates.

Another way of accomplishing the task of choosing a proper potential is to reconstruct it from the observed spectra [7], but again the low accuracy of measurements as well as the fact that the reconstruction is based on a Taylor expansion of the potential (with higher order derivatives given in dependence of the amount and quality of observational data), implies a large uncertainty in the outcomes of the standard reconstruction procedure, from the point of view of the potential uniqueness [7].

Anticipating the near-future launch of satellites capable of measuring microwave background anisotropies to an accuracy of a few percent or better, across a wide range of angular scales [8], an assessment of the accuracy of predictions of the anisotropies for given cosmological models has been stressed. Grivell and Liddle [9] have confirmed that for most models of inflation, the Stewart and Lyth analytic calculations [10] should give extremely accurate predictions.

Lyth and Stewart [11] began with the precise calculation for power-law inflation [12] and then they went on to use this exact result to analytically compute the next-order slow-roll correction to the standard formula [10]. At this level of approximation, the Stewart and Lyth equations for the spectral indices [10] can be rewritten as non-linear differential equations in terms of the first slow-roll parameter ϵ [13,14]. Hence, a third option for the determination of the inflationary potential, that we shall discuss in this paper, is to use observational information about density perturbations and gravitational waves spectra as input in these differential equations, to solve for ϵ and to find the corresponding inflationary potential. We call this procedure the *Stewart–Lyth inverse problem*.

In this work, after introducing the Stewart–Lyth inverse problem, we test the feasibility of the method by finding the proper potential for the well-known scenario of power-law inflation. Nevertheless, the involved system of differential equations composed by a second order and a first order equations, have proved to be very difficult to solve for general functional forms of the perturbations spectra. Taking this into account, in this paper we restrict our analysis to a qualitative study of the dynamics described by these equations. To draw conclusions about the behaviour of the general solutions, the equations are studied using the spectral indices as parameters. For the corresponding reduced equations, we analyze the phase space for the second order equation which presents a singularity that strongly determines the flow geometry. Not cyclical orbits are found. The reduced first order equation is solved for any value of the tensorial spectral index and the possible behaviours are analyzed with all of the solutions being monotonic. Except in the case of null tensorial index, the singularity is also observed. In general, for solutions of the Stewart–Lyth inverse problem with smoothly and slowly changing spectral indices, periodic, quasi-periodic or chaotic general solutions should not be expected. The theoretical analysis as well as observations suggest that power-law solutions are still valid.

In the next Sec. we briefly describe the theoretical frame for the Stewart–Lyth calculations and present their originally algebraic equations in terms of the spectral indices. In Sec. III we introduce the Stewart–Lyth inverse problem. Sec. IV is devoted to the qualitative analysis of the phase-spaces of the reduced second order equation for the first slow-roll

parameter. The analysis of the solutions for the reduced first order equation is presented in Sec. V. We summarize the main results obtained in Sec. VI.

II. THE STEWART–LYTH EQUATIONS

A. The single scalar field scenario

The theoretical frame for the Stewart–Lyth calculation is the flat Friedmann–Robertson–Walker universe containing a single scalar field equivalent to a perfect fluid with equations of motions given by

$$H^2 = \frac{\kappa}{3} \left(\frac{\dot{\phi}^2}{2} + V(\phi) \right), \quad (1)$$

$$\ddot{\phi} + 3H\dot{\phi} = -V'(\phi), \quad (2)$$

where ϕ is the inflaton, $V(\phi)$ is the inflationary potential, $H = \dot{a}/a$ is the Hubble parameter, a is the scale factor, dot and prime stand for derivatives with respect to cosmic time and ϕ respectively, $\kappa = 8\pi/m_{Pl}^2$ is the Einstein constant and m_{Pl} is the Planck mass.

In this framework, the first three slow-roll parameters were respectively defined in [15], we shall write them here as in [7]:

$$\epsilon(\phi) \equiv 3 \frac{\dot{\phi}^2}{2} \left[\frac{\dot{\phi}^2}{2} + V(\phi) \right]^{-1} = \frac{2}{\kappa} \left[\frac{H'}{H} \right]^2, \quad (3)$$

$$\eta(\phi) \equiv -\frac{\ddot{\phi}}{H\dot{\phi}} = \epsilon - \frac{\epsilon'}{\sqrt{2\kappa\epsilon}}, \quad (4)$$

$$\xi(\phi) \equiv \left[\epsilon\eta - \left(\frac{2}{\kappa} \epsilon \right)^{\frac{1}{2}} \eta' \right]^{\frac{1}{2}}. \quad (5)$$

Up to a constant, the first slow-roll parameter (3) is a measure of the relative contribution of the kinetic energy to the total energy of the field. By definition $\epsilon \geq 0$, and because inflation can be defined as $\ddot{a} > 0$, for inflation to proceed: $\epsilon < 1$.

B. Power–law inflation

Few models of inflation allow to exactly calculate scalar and tensorial perturbations. One of them is the power–law model [12], a particular scenario of inflation where:

$$a(t) \propto t^p, \quad (6)$$

$$H(\phi) \propto \exp \left(-\sqrt{\frac{\kappa}{2p}} \phi \right), \quad (7)$$

$$V(\phi) \propto \exp \left(-\sqrt{\frac{2\kappa}{p}} \phi \right), \quad (8)$$

with p being a positive constant. It follows from (3), (4), and (5) that in this case the slow-roll parameters are constant and equal each other.

C. The indices equations

Exact expressions for the asymptotic scalar (density perturbations) and tensorial (gravitational waves) power spectra for the case of power-law inflation was correspondingly derived by Lyth and Stewart [11] and Abbot and Wise [16].

Assuming that the deviation of the higher slow-roll parameters from ϵ is small (power-law approximation) and that ϵ is small with respect to unity (slow-roll approximation), Stewart and Lyth [10] derived next-to-leading order expressions for both spectra. In terms of the spectral indices, these expressions are

$$1 - n_s(k) \simeq 4\epsilon - 2\eta + 8(C + 1)\epsilon^2 - (10C + 6)\epsilon\eta + 2C\xi^2, \quad (9)$$

$$n_T(k) \simeq -2\epsilon [1 + (2C + 3)\epsilon - 2(C + 1)\eta], \quad (10)$$

where the notation is that of [7]; $n_s(k)$ and $n_T(k)$ are the scalar and tensorial spectral indices respectively, k is the wave number of the comoving scale, and $C \approx -0.73$ is a constant related to the Euler constant originated in the expansion of Gamma function. The symbol \simeq is used to indicate that these equations were obtained using the power-law and slow-roll approximations. Hereafter we shall use the $=$ sign in our calculations, but the meaning of approximation should be added whenever it applies.

For a giving expression of the scale factor, the Hubble parameter and the potential are determined, and then by substituting definitions (3), (4), and (5) in the Stewart–Lyth equations (9) and (10), the scale-dependent spectral indices are obtained. For instance, giving (7) and substituting in (3), (4), and (5), one obtains $\epsilon = \eta = \xi = 1/p$, which in turn substituted in (9) and (10) yield $n_s - 1 = n_T = \text{const.}$. This is an alternative definition for power-law inflation. We should note that the spectral indices are directly related with the power spectra (for details see [7]).

III. FORMULATION OF THE STEWART–LYTH INVERSE PROBLEM

In this section we shall formulate a method for finding the inflaton potential using observational information on the spectral indices. Denoting $T \equiv \dot{\phi}^2/2$ and using definitions (3), (4), (5), together with equations (1) and (2) then, in a straightforward manner, we obtain:

$$\epsilon = 3\frac{T}{T + V} = \frac{\kappa T}{H^2}, \quad (11)$$

$$\eta = \kappa \frac{dT}{dH^2}, \quad (12)$$

$$\xi^2 = \kappa\epsilon \frac{dT}{dH^2} + 2\kappa\epsilon H^2 \frac{d^2T}{d(H^2)^2}. \quad (13)$$

Defining $\tau \equiv \ln H^2$, $\delta(k) \equiv n_T(k)/2$ and $\Delta(k) \equiv (n_s(k) - 1)/2$, and substituting (11), (12), and (13) in (9) and (10), the indices equations in terms of the first slow-roll parameter ϵ and its derivatives with respect to τ ($\hat{\epsilon} \equiv d\epsilon/d\tau$ and $\hat{\hat{\epsilon}} \equiv d^2\epsilon/d\tau^2$) become:

$$2C\epsilon\hat{\epsilon} - (2C + 3)\epsilon\hat{\epsilon} - \hat{\epsilon} + \epsilon^2 + \epsilon + \Delta = 0, \quad (14)$$

$$2(C + 1)\epsilon\hat{\epsilon} - \epsilon^2 - \epsilon - \delta = 0. \quad (15)$$

The second order non-linear differential equation (14) was first introduced in [13], while the first order equation (15) was derived first in [14]. Notice that equations (14) and (15) are just alternative representations of the Stewart–Lyth equations (9) and (10). The approach of [13] for the potential reconstruction is incomplete because is restricted to the case $\Delta(k) = \text{const.}$, and, on the other hand, the equation for the tensorial spectral index (15) is considered only in the trivial case of power–law inflation [14]. As we shall see, the equation (15) imposes rigorous constraints upon the set of solutions of (14).

By the *Stewart–Lyth inverse problem* we mean the problem consisting in solving equations (14) and (15) for ϵ , given expressions for the spectral indices, and finding the corresponding inflaton potential using the definitions of the first slow–roll parameter (3) and (11). We prefer this denomination instead of “reconstruction” because we will use explicit functional forms of the spectra as input in the problem and correspondingly we will obtain functional forms for the potentials rather than pieces of information about them.

As was already mentioned, having an expression for $\epsilon(\tau)$ the corresponding potential as a function of τ can be obtained from (11):

$$V(\tau) = \frac{1}{\kappa} [3 - \epsilon(\tau)] \exp(\tau). \quad (16)$$

On the other hand, taking into account that $\dot{\phi} = \dot{\tau} \dot{\phi}$ and using (3), the scalar field as a function of τ is given by,

$$\phi(\tau) = -\frac{1}{\sqrt{2\kappa}} \int \frac{d\tau}{\sqrt{\epsilon(\tau)}} + \phi_0, \quad (17)$$

where ϕ_0 is an integration constant.

Finally, the inflationary potential as parametric function of the inflaton can be given:

$$V(\phi) = \begin{cases} \phi(\tau), \\ V(\tau). \end{cases} \quad (18)$$

The above expressions are similar to those used in [13] but we would like to stress that the functional form for ϵ in expressions (16) and (17) must be solution of both (14) and (15).

As a simple example of a resolution of the Stewart–Lyth inverse problem, let us analyze the case of power–law inflation, where the spectral indices are constants. Substituting (15) in (14) with constant Δ and δ , an algebraic equation for ϵ is obtained. Since the coefficients of this equation are scale–independent, all the solutions for this algebraic equation are just of the form: $\epsilon = 1/p$ with $p = \text{const.}$ Substituting this expression for ϵ in (17) and after some algebra, we obtain for the Hubble parameter:

$$H(\phi) = \exp \left(-\sqrt{\frac{\kappa}{2p}} (\phi - \phi_0) \right). \quad (19)$$

We can see that, up to a constant, (19) is equivalent to (7). Now, substituting $\epsilon = 1/p$ and H^2 in (16), we obtain,

$$V(\phi) = \frac{3p - 1}{\kappa p} \exp \left(-\sqrt{\frac{2\kappa}{p}} (\phi - \phi_0) \right), \quad (20)$$

in complete correspondence with (8).

On the relevance of taking into account the first-order equation, we want to remark that, although equation (14) has a large number of solutions for a constant scalar index, once equation (15) with $\delta = \text{const.}$ was used as a first integral of (14), the unique remaining solution is just the potential given by (20).

Even for a scale-independent scalar spectrum, equation (14), when it is taken with no regards to (15), has proved to be very difficult to be analytically solved; solutions have been found only for a few fixed values of Δ (see [14,17] and references therein). This obstacle is even harder to overcome when an scale-dependent scalar spectrum is assumed; even for the first order equation (15) it is hard to find an explicit solution for ϵ for any value of $\delta = \text{const.}$, and even more difficult for $\delta = \delta(\tau(k))$.

In the present work, we will focus in the dynamical aspect of the Stewart–Lyth inverse problem, i.e., in the dynamics of the first slow-roll parameter determined by equations (14) and (15). The problem of integrating for the inflationary potential is left to be done in a near future.

IV. PHASE SPACES ANALYSIS OF THE REDUCED SECOND ORDER EQUATION

For an understanding of the dynamics behind equations (14) and (15), the best approach seems to be a qualitative analysis of the corresponding phase-spaces.

Not having yet an explicit expression for $\Delta(\tau)$ and $\delta(\tau)$, we use the following approach in order to draw conclusions about the dynamics described by (14) and (15): if we consider $\Delta(\tau)$ and $\delta(\tau)$ as the forcing element in these equations, then we can assume the dynamics to be characterized by one more dimension. The $(\epsilon, \hat{\epsilon})$ planes $((\tau, \epsilon)$ for the first order equation) corresponding to the different values of this new coordinate are transverse to the trajectories given by these equations. Having the phase-portraits on the planes $(\epsilon, \hat{\epsilon})$ for any value of $\Delta = \text{const.}$ in equation (14) and the solutions (τ, ϵ) for any $\delta = \text{const.}$ in equation (15), the geometry of the surfaces along which the real trajectories spread out could be outlined, assuming slow variation for $\Delta(\tau)$ and $\delta(\tau)$.

Hereafter, we will refer to equations (14) and (15) with constant Δ and δ as the **reduced** equations of the Stewart–Lyth inverse problem, and the space for solutions depending on τ as the **extended** phase-space.

Solutions for the reduced first order equation (15) will be studied in the next section. Let us now proceed with the analysis of the dynamics given by (14). This equation can be rewritten as

$$\hat{\epsilon} - \frac{1}{2C} \left(2C + 3 + \frac{1}{\epsilon} \right) \hat{\epsilon} + \frac{1}{2C} \left(\epsilon + 1 + \frac{\Delta}{\epsilon} \right) = 0. \quad (21)$$

With the change of variables

$$\begin{cases} x_1 = \epsilon, \\ x_2 = \hat{\epsilon}, \end{cases} \quad (22)$$

we obtain the system:

$$\begin{cases} \hat{x}_1 \equiv F(x_1, x_2) = x_2, \\ \hat{x}_2 \equiv G(x_1, x_2) = -\frac{1}{2C} \left(x_1 + 1 + \frac{\Delta}{x_1} \right) + \frac{1}{2C} \left(2C + 3 + \frac{1}{x_1} \right) x_2. \end{cases} \quad (23)$$

For $\Delta = \text{const.}$, the condition for existence of solution [18], i.e., the continuity condition for the vector field, holds at every point $(x_1, x_2) \in \mathcal{P} \equiv \mathbb{R}^2 \setminus \{(0, x_2), \forall x_2\}$. On the other hand,

$$|G(x_1, x_2^{(1)}) - G(x_1, x_2^{(2)})| = \frac{1}{2|C|} \left| (2C + 3) + \frac{1}{x_1} \right| |x_2^{(1)} - x_2^{(2)}|, \quad (24)$$

where the upper indices denote any two different values of x_2 . Then, the uniqueness condition, i.e., Lipschitz condition, holds for the same set \mathcal{P} . Therefore, unique solution for (23) certainly exists at any point in \mathcal{P} . In a similar fashion, the differentiability of solution with respect to initial conditions and parameters of the system is also satisfied. Hence, we can use the results of qualitative theory of dynamical systems in the plane for the study of (23) [19].

The set of singular points of (23) is the union of the set of fixed points ($F = G = 0$) and the x_2 -axis. We should note that around point $p_s = (0, \Delta)$ the field is well defined along directions for which $x_2 \rightarrow \Delta$ faster than $x_1 \rightarrow 0$. This case will be analyzed in detail in Subsec. IV C.

A. Fixed points

The fixed points of this system are the set $\{(x_1, x_2)\}$ such that:

$$\begin{aligned} F(x_1, x_2) &= 0, \\ G(x_1, x_2) &= 0. \end{aligned}$$

Therefore $x_2 = 0$. From $G(x_1, x_2) = 0$ and for $x_1 \neq 0$, we have

$$x_1^2 + x_1 + \Delta = 0. \quad (25)$$

The roots of this quadratic polynomial are

$$\alpha_{\pm} = -\frac{1}{2} \pm \frac{\sqrt{1 - 4\Delta}}{2}, \quad (26)$$

where the symbol α_{\pm} stands for the two different roots of equation (25). These roots are placed symmetrically with respect to $x_1 = -0.5$. From now on we shall use the symbol α without lower indices while referring to any of these roots.

According to the Grobman–Hartman theorem [20], the local behavior near the equilibrium position depends on the linear part (if exists) of the vector field, in those cases where the eigenvalues of the Jacobian matrix of the vector field associated to the system have non zero real part. Hence, in order to develop local analysis of the equilibrium positions, we calculate:

$$J(x_1, x_2) = \begin{pmatrix} 0 & 1 \\ \frac{1}{2C} \left(-1 + \frac{\Delta - x_2}{x_1^2} \right) & \frac{1}{2C} \left(2C + 3 + \frac{1}{x_1} \right) \end{pmatrix}. \quad (27)$$

Because the equilibrium positions are of type $(\alpha, 0)$ the Jacobian matrix in these points is written as

$$J(\alpha, 0) = \begin{pmatrix} 0 & 1 \\ g_1 & g_2 \end{pmatrix}, \quad (28)$$

where:

$$g_1 = \frac{1}{2C} \left(\frac{\Delta}{\alpha^2} - 1 \right), \quad (29)$$

$$g_2 = \frac{1}{2C} \left(2C + 3 + \frac{1}{\alpha} \right). \quad (30)$$

The characteristic polynomial, corresponding to the eigenvalue problem of (28), is

$$p(\lambda) = \lambda^2 - g_2\lambda - g_1, \quad (31)$$

with roots,

$$\lambda_{\pm} = \frac{1}{2}g_2 \pm \frac{1}{2}\sqrt{g_2^2 + 4g_1}. \quad (32)$$

We study the possible behavior near the equilibrium positions depending on the values of the polynomial roots (32). For a complete discussion, definitions and main results, see [18–20]. In general, one is concerned about whether the eigenvalues are real or complex, and if their real parts are greater, equal or less than zero.

The roots (32) depend on the value of discriminant $D = g_2^2 + 4g_1$; they will be real if $D \geq 0$. Hence, the following inequality holds:

$$D = 1 + \frac{1}{C} + \left(\frac{3}{2C} \right)^2 + \left(\frac{1}{C} + \frac{3}{2C^2} \right) \frac{1}{\alpha} + \left(\frac{1}{4C^2} + \frac{2\Delta}{C} \right) \frac{1}{\alpha^2} \geq 0. \quad (33)$$

This inequality can be written as

$$[(2C + 3)^2 - 8C]\alpha^2 + 2(2C + 3)\alpha + 8C\Delta + 1 \geq 0. \quad (34)$$

The polynomial in (34) has roots:

$$\alpha_{+,-} = \frac{-(2C + 3) \pm 2\sqrt{2C(1 - [(2C + 3)^2 - 8C]\Delta)}}{(2C + 3)^2 - 8C}. \quad (35)$$

We shall see soon that the fixed point $(\alpha_-, 0)$ is always a saddle point. Hence, the current analysis has sense only for α_+ . Comparing the expressions for this root given by (26) and (35), solving for Δ and substituting the value of $C \approx -0.73$, we find out that roots (32) are real if and only if $\Delta \leq 0.124273$.

Now we are able to classify the fixed points. For $\Delta > 0.25$, case *a*), there are not fixed points and the flow is deformed from a laminar one only near the point p_s (see Fig. 1, case *a*) and subsection IV C). Hereafter, in the Figs. we represent the flow direction by means of arrows.

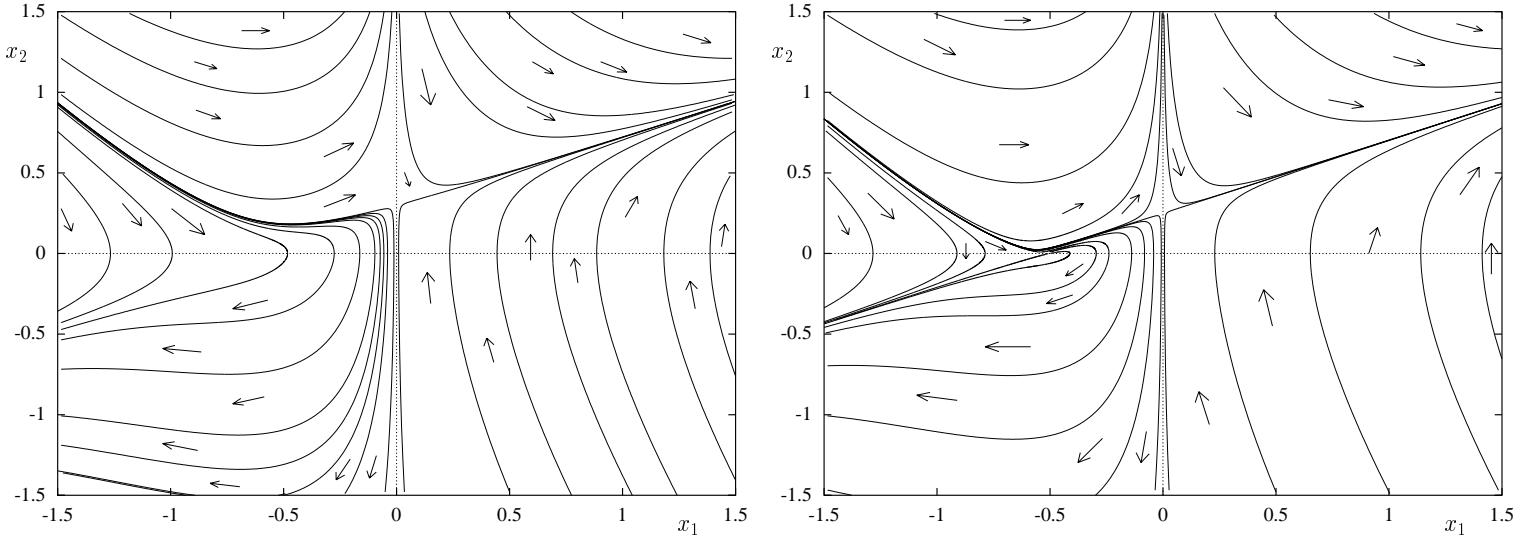


FIG. 1. Reduced phase portraits for $\Delta = 0.3$, case *a*), and for $\Delta = 0.25$, case *b*).

For $\Delta = 0.25$, case *b*), one of the eigenvalues has zero real part and hence the stability of the unique and degenerated fixed point $(-0.5, 0)$ cannot be determined by linearization. The remaining eigenvalue has positive real part, then the local behavior transverse to the center manifold is controlled by the exponentially expanding flows in the local unstable manifold. According to Center Manifold theorem for flows [19], the center manifold (it could be not unique) is tangent at $(-0.5, 0)$ to the center subspace that, in this case, coincides with the x_1 -axis. On the other hand, the unstable manifold is tangent to the unstable subspace, i.e., the line $x_2 = g_2 x_1$ with g_2 , for this case, being $(2C + 1)/2C \simeq 0.315068$ (Fig. 1, case *b*)). We recall that each subspace is spanned by the eigenvectors corresponding to eigenvalues (32).

Further, for $\Delta < 0.25$ and $\Delta \neq 0$ we have two non-degenerate fixed points over the x_1 -axis symmetrically distributed with respect to $x_1 = -0.5$.

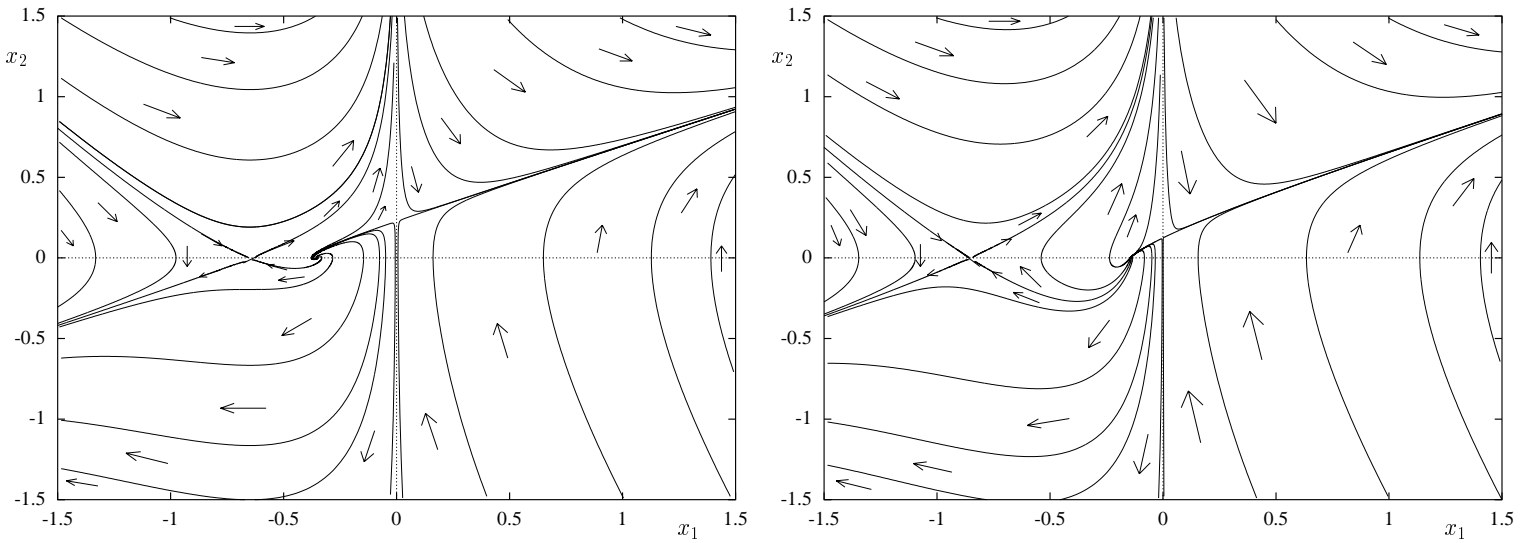


FIG. 2. Reduced phase portrait for $\Delta = 0.227694$, case *c*), and for $\Delta = 0.124273$, case *d*).

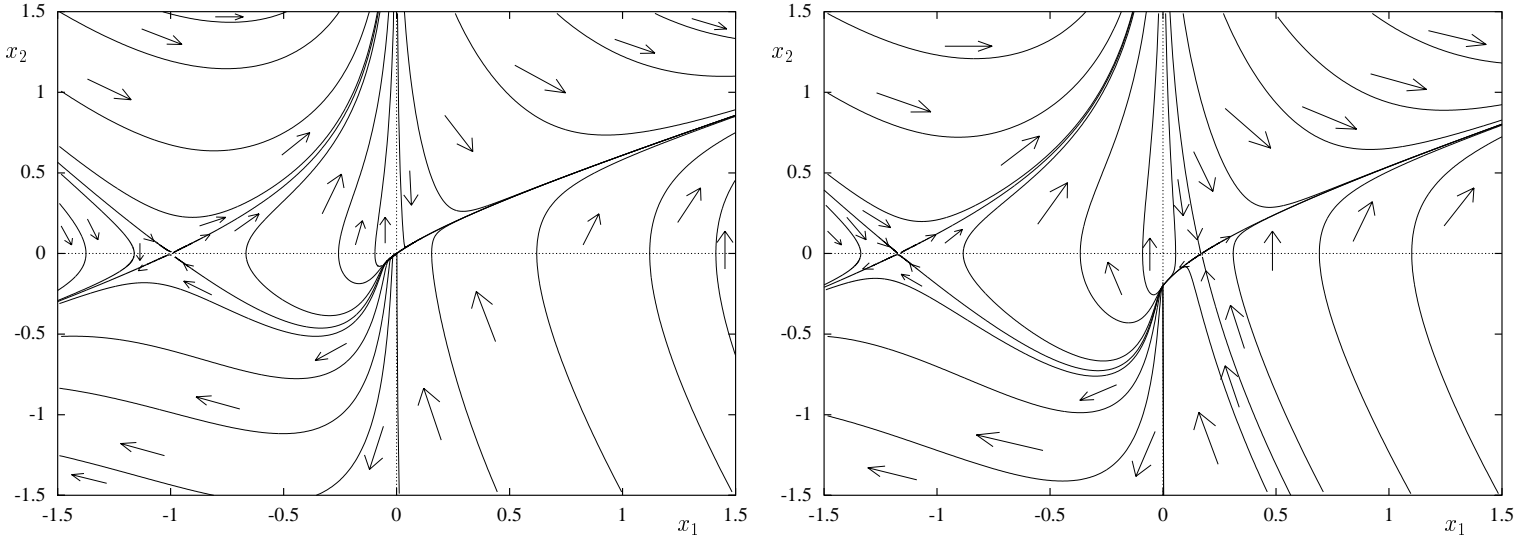


FIG. 3. Reduced phase portrait for $\Delta = 0$, case *e*), and for $\Delta = -0.2$, case *f*).

Let us proceed with the fixed points classification paying attention to the leftmost one. Obviously, the value of α_- for this point is always negative for any Δ and hence $g_1 > 0$. This way, the leftmost fixed point is always a saddle. The rate $|\lambda_+| / |\lambda_-|$ is equal to 1 for $\Delta = -0.25 + 2(C+1)/(2C+3) \simeq 0.227694$, value of Δ that corresponds to $\alpha_+ = -0.64935$. For Δ greater (less) than 0.227694 the trajectories converge to the saddle point faster (slower) than they diverge from it.

For the rightmost fixed point the situation is richer. First, from (30) one can see that $g_2 > 0$ for any $\Delta < 0.25$ and $\Delta \neq 0$. For $0 < \Delta < 0.25$ we have $g_1 < 0$, then in the interval $0.124273 < \Delta < 0.25$, case *c*), the rightmost fixed point is an unstable focus (Fig. 2).

As can be observed in the figure, one of the stable separatrices of the saddle point seems to be directly spiraling out from the focus. For $0 < \Delta \leq 0.124273$, case *d*), the rightmost fixed point is an unstable node (Fig. 2). In the case $\Delta = 0$, case *e*), $g_2 < 0$ and we have a single saddle located at $(-1, 0)$ (see Fig. 3). For $\Delta < 0$, case *f*), the rightmost fixed point becomes a saddle (Fig. 3) located on the right half-plane.

B. Closed orbits

Note that the sign of the vector field divergence for (23) does not depend on Δ , thus the value of the parameter is of no importance while applying the Bendixson criterion [19], which states that no closed path can be found in plane regions where the vector field divergence is null or not undergoes sign changes. This criterion, applied to (23), divides the plane in four regions without divergence sign changes:

$$\begin{cases} \mathcal{P}_1 \equiv \{(x_1, x_2); x_1 > 0, \forall x_2\}, \\ \mathcal{P}_2 \equiv \{(x_1, x_2); -0.64935 < x_1 < 0, \forall x_2\}, \\ \mathcal{P}_3 \equiv \{(-0.64935, x_2); \forall x_2\}, \\ \mathcal{P}_4 \equiv \{(x_1, x_2); x_1 < -0.64935, \forall x_2\}, \end{cases}$$

with diverging vector field,
 with a converging vector field,
 with null divergence, and
 with positive divergence.

It is worthy to note that, even if both half-planes ($x_1 < 0, x_1 > 0$) are connected

through point p_s , this connection should take place in one and only one direction. This way, no closed orbit could be found in regions \mathcal{P}_1 and \mathcal{P}_3 or entirely lying in \mathcal{P}_2 or \mathcal{P}_4 . Any closed trajectory should belong to $\mathcal{P}_2 \cup \mathcal{P}_3 \cup \mathcal{P}_4$. Then, three possible scenarios with closed path could take place. First, a homoclinic orbit (i.e., a saddle connection) enclosing the second fixed point (focus or node, we will refer to it as α_+). The second possibility is a limit cycle to which converges all of the trajectories starting from α_+ and from which spiral out the orbits. Finally, it could be possible to find a homoclinic orbit with an embedded limit cycle around α_+ . Each of these scenarios has two possible realizations depending on whether both fixed points lie in \mathcal{P}_2 or the saddle lies in \mathcal{P}_4 and α_+ lies in \mathcal{P}_2 . The realizations for the more general scenario (a homoclinic orbit with an embedded limit cycle) are schematically represented in Figs. 4.

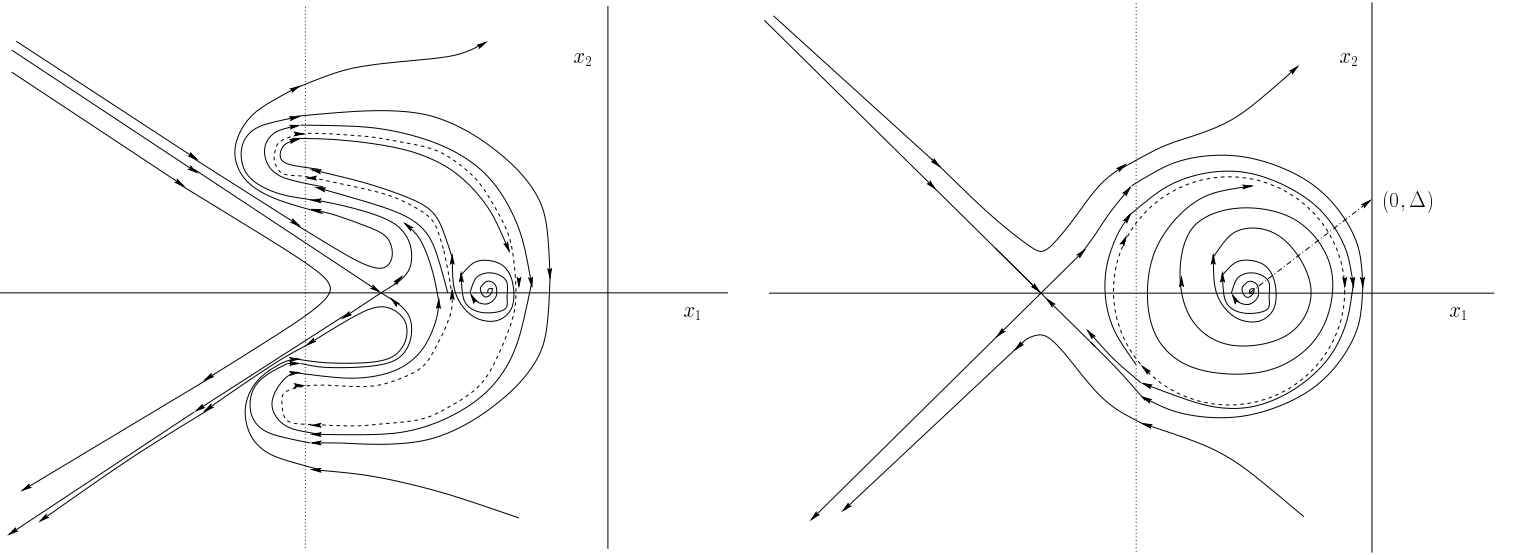


FIG. 4. Scheme of a homoclinic orbit with an embedded limit cycle. The curve (---) represents the limit cycle and the trajectory given by equation 36. The line (···) is $x_1 = -0.64935$.

One conclude from the left scheme in Fig. 4 that not closed trajectory will be found with both fixed points lying in \mathcal{P}_2 because sign changes in the derivative for the vector field along x_1 , at each side of axis $x_2 = 0$, are not allowed by the first equation of (23). With regards to the realization plotted on the right part of Fig. 4, we shall see in subsection IV C that for this range of x_1 there is a trajectory (represented by the line (···) on the Fig.) that can be fairly approximated by

$$x_2 = \left(1 - \frac{x_1}{\alpha_+}\right) \Delta, \quad (36)$$

then no closed orbit can neither exists here.

C. Flow near point p_s

As we have already mentioned, a sharp feature of these phase spaces is the collisions of the trajectories with the border $x_1 = 0$. Our system possess here a vector field discontinuity

that strongly determines the behaviour of the trajectories near this border. Such a piecewise continuous map is a more general system than those piecewise differentiable maps previously reported and analyzed in literature (see for example: [21,22]).

A particularly interesting situation is exhibited by the trajectories near the point $p_s = (0, \Delta)$. First of all, let us note that no statement can be done about the existence or uniqueness of solutions of (23) at this point. To analyze the behaviour of the flow in the neighborhood of this point we rewrite the system as,

$$\hat{x}_1 = x_2, \quad (37)$$

$$\hat{x}_2 = \frac{1}{2C} \left\{ (3 + 2C)\Delta - x_1 - 1 + [(3 + 2C)x_1 + 1] \frac{(x_2 - \Delta)}{x_1} \right\}. \quad (38)$$

We shall look for a solution $x_2 = \Delta + f(x_1)$ for the phase curves in the neighborhood of the above mentioned point. Differentiating this expression with respect to x_1 , taking into account that $\hat{x}_2 = \hat{x}_1 dx_2/dx_1 = x_2 df/dx_1$, substituting in (37) for the approximation $x_1 \ll 1$ and $f(x_1) \ll 1$ ($x_2 \approx \Delta$), we obtain the following non-homogeneous linear equation for $f(x_1)$:

$$\frac{df}{dx_1} - \frac{1}{2C\Delta} \frac{f}{x_1} = \frac{(3 + 2C)\Delta - 1}{2C\Delta}. \quad (39)$$

For $\Delta \neq 1/2C$ the solution of (39) is

$$f(x_1) = \left(1 - \frac{3\Delta}{1 - 2C\Delta} \right) x_1 + K x_1^{1/2C\Delta}, \quad (40)$$

while for $\Delta = 1/2C$,

$$f(x_1) = \frac{3}{2C} x_1 \ln x_1 + K x_1, \quad (41)$$

where K is an integration constant depending on the initial conditions. Hence, the behaviour around the point p_s is described by the following family of curves

$$x_2 = \begin{cases} \Delta + \left(1 - \frac{3\Delta}{1 - 2C\Delta} \right) x_1 + K x_1^{1/2C\Delta}, & \text{if } \Delta \neq 1/2C, \\ \frac{1}{2C} + \frac{3}{2C} x_1 \ln x_1 + K x_1, & \text{if } \Delta = 1/2C. \end{cases} \quad (42)$$

Concerning the qualitative behaviour of the trajectories near the point p_s there are four interesting intervals of Δ . First, for $|\Delta| \gg 1$ the flow seems to ignore the existence of the special singular point $(0, \Delta)$. All the trajectories flows to (or from) the x_2 -axis along parallel lines with slope $1 + 3/2C \simeq -1.054794$. From these lines only that intercepting the x_2 -axis at p_s could arrive to or depart from this point. For positive (but not too large) Δ the trajectories have the distribution observed in the left part of Fig. 5. In this figure we present the case $\Delta = 1/(3 + 2C) \simeq 0.64935$ where the line with $K = 0$ coincides with the stationary solution for x_1 . Then, for $\Delta > 0$ one and only one trajectory could arrive to singular point p_s and one and only one trajectory could leave it. It is precisely this trajectory which can be represented by (36) for $-0.64935 < \alpha_+ < 0$. For $\Delta = 0$, in the left half-plane, all of the trajectories between the unstable separatrices of the saddle point

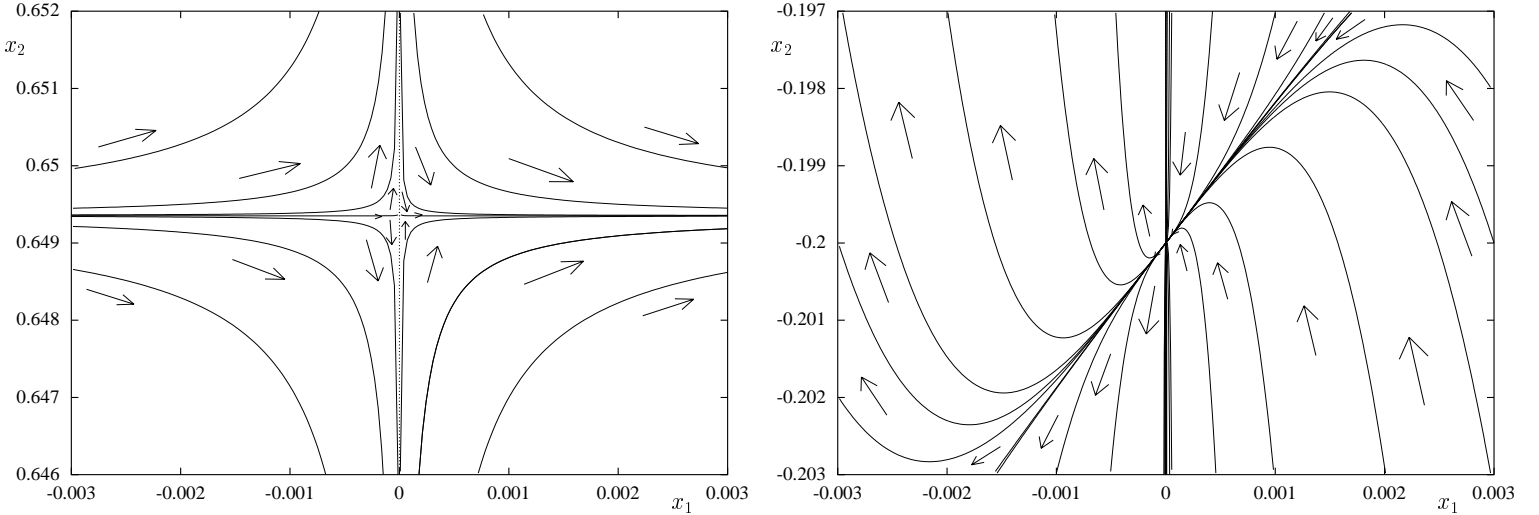


FIG. 5. Flow near the point p_s for $\Delta > 0$ ($\Delta \simeq 0.64935$), and for $\Delta < 0$ ($\Delta \simeq -0.2$).

and the ordinates axis move away from p_s diverging from the line $x_2 = x_1$. In the right half-plane, all of the trajectories converge asymptotically to the solution that behaves like $x_2 = x_1$ in the neighborhood of p_s (recall Fig. 3, case *e*)). All of the trajectories converge to p_s or diverge from it in the same direction. Finally, in the case of negative Δ (but again with not too large absolute value), the trajectories converge to p_s or diverge from it tangent to the lines $K = 0$ with slope given by (42) (Fig. 5, right part).

V. THE REDUCED FIRST ORDER EQUATION.

We have already stressed the importance of (15) for constraining the possible solutions of (14). Let us consider now the equation:

$$2(C+1)\epsilon\hat{\epsilon} - \epsilon^2 - \epsilon - \delta = 0, \quad (43)$$

with constant δ .

The solutions of this equation also depend on the parameter value. For $\delta > 0.25$, we have

$$\ln \left[\frac{|\epsilon^2 + \epsilon + \delta|}{B} \right] - \frac{1}{\sqrt{\delta - 1/4}} \arctan \left(\frac{\epsilon + 1/2}{\sqrt{\delta - 1/4}} \right) - \frac{\tau}{C+1} = 0, \quad (44)$$

where B is the integration constant.

For $\delta = 0.25$, the solution of (43) is that of the algebraic equation

$$(\epsilon + 1/2)^2 - B \exp \left(\frac{\tau}{C+1} - \frac{1}{\epsilon + 1/2} \right) = 0. \quad (45)$$

Now, for $\delta < 0.25$, and $-0.5 - 0.5\sqrt{1-4\delta} < \epsilon(\tau) < -0.5 + 0.5\sqrt{1-4\delta}$, the solution is obtained from

$$|\epsilon^2 + \epsilon + \delta| - B \left(\frac{\sqrt{1-4\delta} - 2\epsilon - 1}{\sqrt{1-4\delta} + 2\epsilon + 1} \right)^{\frac{1}{\sqrt{1-4\delta}}} \exp \left(\frac{\tau}{C+1} \right) = 0, \quad (46)$$

and, for $\delta < 0.25$ but $\epsilon(\tau) < -0.5 - 0.5\sqrt{1-4\delta}$ and $\epsilon(\tau) > -0.5 + 0.5\sqrt{1-4\delta}$, the solution results from,

$$|\epsilon^2 + \epsilon + \delta| - B \left(\frac{2\epsilon + 1 - \sqrt{1-4\delta}}{2\epsilon + 1 + \sqrt{1-4\delta}} \right)^{\frac{1}{\sqrt{1-4\delta}}} \exp \left(\frac{\tau}{C+1} \right) = 0. \quad (47)$$

Note that the solution for $\delta = 0$ is a special case of (47), i.e.,

$$\epsilon(\tau) = (\epsilon_0 + 1) \exp \left(\frac{\tau}{2(C+1)} \right) - 1, \quad (48)$$

where ϵ_0 is the initial condition.

Possible behaviours of solutions of (43) for different values of δ are summarized in Fig. 6. The five interesting intervals are represented by vertical bands in the above plot. In each

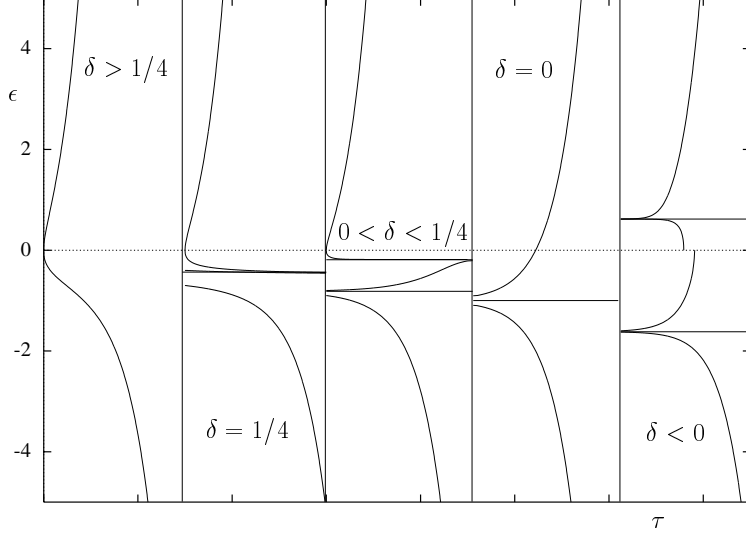


FIG. 6. Solutions of the reduced first order equation for different values of δ . In each of the five regions divided by vertical lines typical solutions for δ in the corresponding interval are presented. In every region each curve branch that goes from left to right is a solution with different initial values.

band the curves branch spreading from left to right is a solution starting from a different initial condition. We can see that all of the solutions are monotonic. In some cases they evolve unbounded, in some other cases bounded by the stationary solutions given by the roots of

$$\epsilon^2 + \epsilon + \delta = 0.$$

VI. CONCLUSIONS

We introduced the Stewart–Lyth inverse problem as the determination of the inflaton potential through expressions for the first slow-roll parameter obtained as a solution of differential equations. These equations were derived from the Stewart–Lyth equations for the spectral indices. We tested the feasibility of the method by solving the problem with constant spectral indices as input, corresponding with power-law inflation.

To draw conclusions about the behaviour of general τ –depending solutions we analyze reduced equations using the spectral indices as parameters. The phase space for the reduced second order equation is richer than the generic ones, particularly due to the singularity $\epsilon = 0$ and to the existence of the special singular point $(0, 0.5(n_s - 1))$ near which the flow is deformed even when there are not fixed points. Do not exist cyclical orbits given by the reduced second order equation for any value of n_s . The condition for the existence of stationary solutions with positive first slow-roll parameter is $n_s < 1$, and there is only one such a solution for every constant value of the scalar spectral index.

The reduced first order equation was solved for any value of the tensorial spectral index. Five possible behaviours were found for the solutions: stationary, asymptotically increasing, asymptotically decreasing, boundlessly increasing, and boundlessly decreasing. The singularity $\epsilon = 0$ was also observed, except in the case $n_T = 0$. The condition for the existence of stationary solutions with positive first slow-roll parameter is $n_T < 0$, and there is only one such a solution for every constant value of the tensorial spectral index.

In general, for solutions of the Stewart–Lyth inverse problem with smoothly and slowly changing spectral indices in the expected range of values, we shall find that the trajectories would be confined in one of the sectors of the extended phase space divided by the axis $\epsilon = 0$. The exception could be those system with the tensorial index crossing through value $n_T = 0$ while the scalar index is greater than 1. Due to the lack of periodic solutions for the reduced equations, periodic, quasi-periodic or chaotic extended solutions should not be expected. Suitable (and unique in each case) power-law solutions will exist if and only if $n_s < 1$ and (consistently with the definition of power-law inflation) $n_T < 0$. Taking this last result into account, estimations of the scalar index based in the recent observations by the collaborations BOOMERANG and MAXIMA–1 [1,2] indicate that, despite its simplicity, power-law scenario is still a good candidate for the inflationary stage of the early universe.

A great inside about general properties of scale-dependent solutions for smoothly and slowly changing spectral indices was gained in this work. Further efforts will be focus on obtaining solutions for the Stewart–Lyth inverse problem, i.e., explicit functional forms of the inflationary potential.

ACKNOWLEDGMENTS

This research is supported in part by the CONACyT grant 32138–E and the Sistema Nacional de Investigadores (SNI). The work of one of the authors (RM) was partially supported by project DGAPA IN122498. We want to thank Andrew Liddle and Eckehard Mielke for helpful discussions.

REFERENCES

- [1] P. de Bernardis *et al.*, *Nature* **404**, 955 (2000); A.E. Lange *et al.*, [astro-ph/0005004](#) (2000).
- [2] S. Hanany *et al.*, [astro-ph/0005123](#); A. Balbi *et al.*, [astro-ph/0005124](#).
- [3] A.H. Guth, *Phys. Rev. D* **23**, 347 (1981).
- [4] A. Linde, *Phys. Lett. B* **108**, 389 (1982).
- [5] A.R. Liddle and D.H. Lyth, *Phys. Lett. B* **291**, 391 (1992).
- [6] A.R. Liddle and D.H. Lyth, *Phys. Rep. B* **231**, 1 (1993).
- [7] J.E. Lidsey, A.R. Liddle, E.W. Kolb, E.J. Copeland, T. Barreiro and M. Abney, *Rev. Mod. Phys.* **69**, 373 (1997).
- [8] L.A. Page, “Measurements of the Cosmic Microwave Background,” in *Proc. of the Eighteenth Texas Symposium on Relativistic Astrophysics and Cosmology* (Singapore: World Scientific 1998).
- [9] I.J. Grivell and A.R. Liddle, *Phys. Rev. D* **54**, 12 (1996).
- [10] E.D. Stewart and D.H. Lyth, *Phys. Lett. B* **302**, 171 (1993).
- [11] D.H. Lyth and E.D. Stewart, *Phys. Lett.* **274**, 168 (1992).
- [12] F. Lucchin and S. Matarrese, *Phys. Rev. D* **32**, 1316 (1985).
- [13] E.W. Mielke and F.E. Schunck, *Phys. Rev. D* **52**, 2 (1995).
- [14] J. Benítez, A. Macías, E.W. Mielke, O. Obregón, and V.M. Villanueva, *Int. J. Mod. Phys. A* **12**, 2835 (1997).
- [15] A.R. Liddle, P. Parsons and J.D. Barrow, *Phys. Rev. D* **50**, 7222 (1994).
- [16] L.F. Abbot and M.B. Wise, *Nucl. Phys. B* **244**, 541 (1984).
- [17] A. García, A. Macías, and E.W. Mielke, *Phys. Lett. A* **229**, 32 (1997).
- [18] L. Elgoltz, *Ordinary Differential Equations and Variational Calculus* (MIR, Moscow, 1989).
- [19] J. Guckenheimer, Ph. Holmes, *Nonlinear Oscillations, Dynamical Systems and Bifurcations of Vector Fields* (Springer-Verlag, New York, 1983).
- [20] J. Palis, W. de Melo, *Geometric Theory of Dynamical Systems, An Introduction* (Springer-Verlag, New York, 1982).
- [21] H.E. Nusse, and J.A. Yorke, *Physica D* **57**, 39 (1992).
- [22] H.E. Nusse, E. Ott, and J.A. Yorke, *Phys. Rev. E* **49**, 1073 (1994).